# Effect of Shielded Distribution Cables on Lightning-Induced Overvoltages in a Distribution System

Li-Ming Zhou, *Senior Member, IEEE,* and Steven A. Boggs, *Fellow, IEEE*

***Abstract*—Lightning strikes have current risetimes ranging from 0.1 to several $\mu$s and can produce transient overvoltages substantially greater than the BIL of many distribution systems in spite of lightning arresters, the value of which is often compromised by excessive lead lengths. We compute the lightning induced overvoltages over distribution transformers connected through cables to an overhead distribution system as a function of ZnO arrester lead length, lightning current rising time, the type of cable, and the length of cable employed. We also compute the voltage across the top 10% of turns of distribution transformers resulting from the high $dV/dt$ of the voltage incident on the transformers. Two types of cable, TR-XLPE and EPR, were considered. The attenuations of the cables were measured as a function of frequency and these propagation characteristics were modeled in the ATP-EMTP program. The computed data indicate that the arrester lead length, lightning rising time, the type of cable, and the length of cable employed have substantial impact on the overvoltage on transformer and the voltage across the top few turns of the transformer winding. The greater high frequency losses of EPR cable can reduce substantially the lightning-induced overvoltages to which distribution transformers are exposed.**

***Index Terms*—Distribution cable, power cable, surge overvoltages.**

## I. Introduction

FAST transients in power systems can be generated by lightning impulses and switching of devices such as vacuum, air, or $SF_6$ insulated interrupters [1]. In the case of lightning-induced overvoltages in distribution systems, the ultimate overvoltage in the absence of an arrester would be the same as in a transmission system, meaning very large relative to the BIL of the distribution system. Modern arresters limit the voltage early into the rise, which means at very short times. Thus, a 40 kA lightning current waveform with a risetime of 0.2 $\mu$s can result in a voltage waveform across the arrester with a risetime of only 20 ns. In addition, the effect of arrester leads, typically in the range of 1 to 3 m long, can increase the initial voltage across the cable termination by several times, from the range of 40 kV with no leads to 250 kV with 3 m leads (Fig. 1). As a result of these phenomena, a distribution cable connected to an overhead distribution circuit may see transient waveforms in the range of 25 pu (relative to peak ac line-to-ground voltage) with risetimes in the range of 100 ns. In the absence of high frequency cable attenuation, these short risetime, large amplitude transients can cause a large voltage across the first few turns of a transformer winding, leading to turn-to-turn failure. High frequency cable attenuation can reduce the $dV/dt$ of lightning and switching induced transients as a function of distance propagated down the cable, extending the transient risetime by absorbing high frequency energy, thereby reducing the turn-to-turn voltage at the top of the transformer windings connected along the cable. In the present work, we have modeled the distribution circuits shown in Figs. 2 and 3 which were provided by a local utility, and we have computed the voltage across transformers and the transient voltage across the top 10% of the transformer windings. The effects of ZnO arrester lead length, lightning current rising time, the type of cable (TR-XLPE or EPR cable), and the length of cable were evaluated using the ATP-EMTP program.

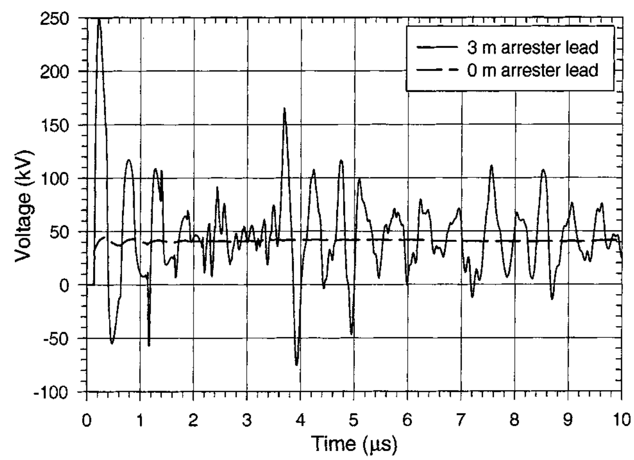


Fig. 1. Waveform across the right-branch cable input for the configuration shown in Fig. 2 for a 15 kV overhead line to cable connection at a riser pole. The lightning current was 40 kA with a risetime of 0.2 $\mu$s. The arresters are gapless. Data are shown for 0 m and 3 m arrester lead lengths.

## II. Cable Attenuation

The attenuation of shielded power cable is caused by three phenomena: 1) skin effect loss of the conductors, 2) dielectric loss of the insulation, and 3) dielectric loss in the semicons. As a result of the large conductors employed in power cables, skin effect losses are normally negligible. For cables insulated with XLPE, which has very low dielectric loss, low frequency

Manuscript received December 27, 1999; revised October 8, 2001.

L.-M. Zhou was with the Electrical Insulation Research Center, University of Connecticut, Storrs, CT 06269-3136 USA. He is now with Tycom, Morristown, NJ 07960 USA (e-mail: lzhou@tycomltd.com).

S. A. Boggs is with the Electrical Insulation Research Center, Institute of Materials Science, University of Connecticut, Storrs, CT 06269-3136 USA and also with the Department of Electrical Engineering, University of Toronto, Toronto, ON M55 1A1, Canada (e-mail: steven.boggs@ieee.org).

Publisher Item Identifier S 0885-8977(02)02754-1.

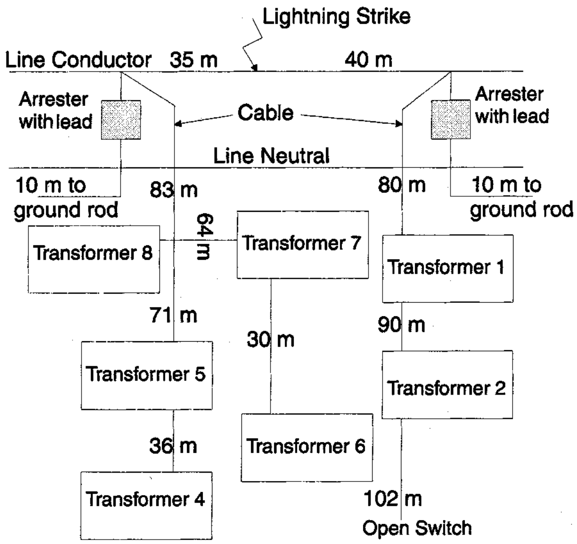


Fig. 2. Section of utility 13.2 kV distribution system which has been modeled. The transformers are modeled as shown in Fig. 3. The cable lengths are labeled in meters.

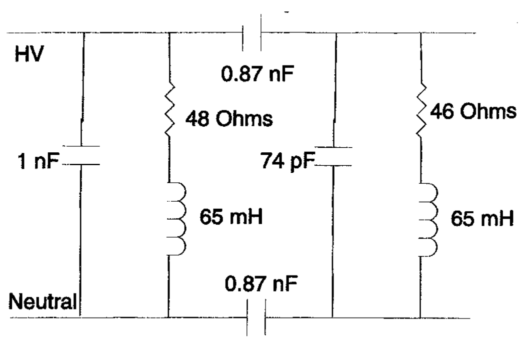


Fig. 3. High frequency electrical model for single-phase distribution transformer [2].

losses are dominated by conductor resistance and dielectric loss while high frequency losses are dominated by dielectric loss in the semicons which results from the propagation of radial displacement current through the resistance of the semicon [3], [4]. This loss is maximum when the resistive impedance of the semicon is equal to its capacitive impedance. Since the resistive impedance is relatively constant with frequency while the capacitive impedance decreases with increasing frequency, the two tend to be equal only in a small range of frequency, usually in the megahertz range. The magnitude of the attenuation is a strong function of the semicon dielectric constant, which is usually in the range of 100 to 2000. Such high dielectric constants result in low attenuations and small contributions to the dielectric loss, as seen in Fig. 4. Fig. 5 shows the attenuation versus frequency and conductor semicon conductivity for a semicon dielectric constant of ten. For a more typical conductor semicon dielectric constant of 100 to 1000, the attenuation would be about one or two orders of magnitude less. Note that although the attenuation (dielectric loss) starts to become appreciable at high frequencies, the attenuation at power frequency caused by the semiconducting shields is totally negligible for any reasonable value of semicon conductivity. This demonstrates that a cable can have appreciable attenuation at high frequency

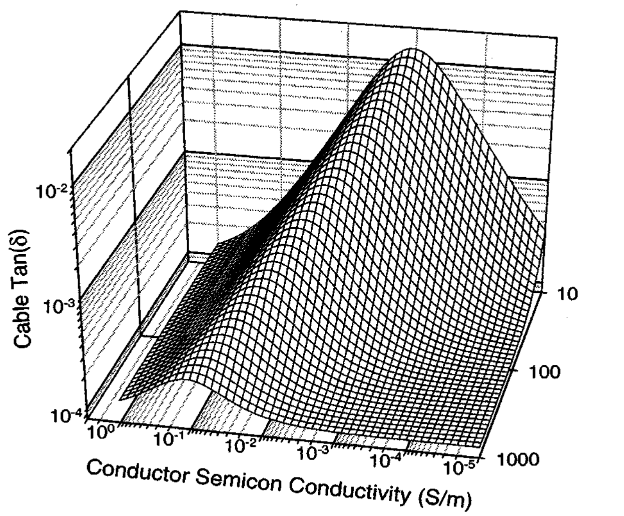


Fig. 4. Cable dielectric loss at 2 MHz as a function of conductor semicon conductivity and dielectric constant for a typical 15 kV class cable geometry. The characteristics of the ground shield semicon are such that they contribute little to the overall cable loss. The loss of the cable insulation is set to 0.001 which limits the lower bound of the cable loss to this value.

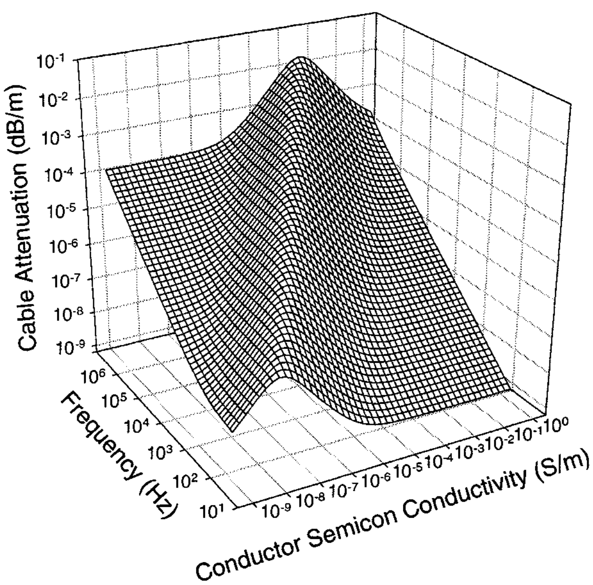


Fig. 5. Cable attenuation as a function of frequency and conductor semicon conductivity for a conductor semicon dielectric constant of ten. Note that the maximum loss is about 0.01 dB/m at 5 MHz and the optimum semicon conductivity. For a more typical semicon dielectric constant of 100, the attenuation would be reduced by about an order of magnitude.

without increasing the attenuation (losses) appreciably at power frequency. Fig. 6 shows the measured attenuations versus frequency for EPR cable and TR-XLPE cable. The TR-XLPE cable has a high frequency attenuation which is in the range caused by semicons. However, the EPR cable has an order of magnitude greater attenuation at high frequencies, in a range which is probably caused by dielectric loss in the insulation.

## III. Distribution Network Model

A section of distribution network provided by a utility is shown in Fig. 2, which consists of single-phase 13.2 kV distribution lines, two riser poles, two ZnO arresters at the riser poles,

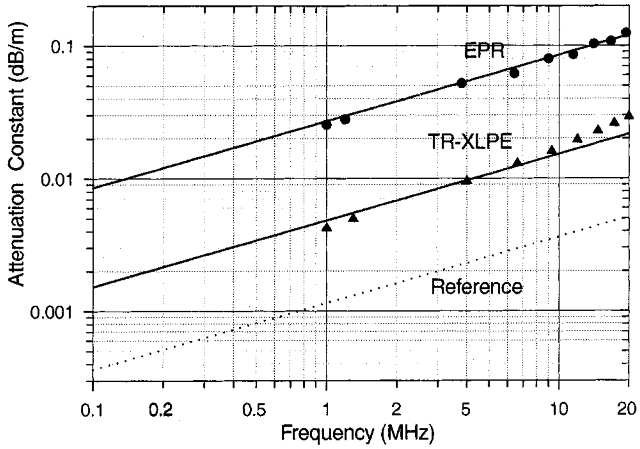


Fig. 6. High frequency attenuation of an EPR cable and a TR-XLPE cable. Symbols provide the data as measured with a high frequency impedance analyzer (HP4191A) while lines provide the calculated loss as implemented in the ATP-EMTP program. The attenuation of EPR cable is about an order of magnitude greater than that of TR-XLPE cable.

shielded power cables and seven distribution transformers. The cables are connected at riser poles, which are fitted with ground leads connected to driven ground rods. Our previous work indicated that the ground rod to earth resistance in the New England area ranges from a few ohms to a few kilohms. In the present model, we have employed the somewhat optimistic value of 50 Ω. The distribution overhead lines are modeled with 150 Ω characteristic impedance, and the riser pole ground leads are modeled as having a 75 Ω characteristic impedance as implemented in the ATP-EMTP using the constant-parameter line model. ZnO arresters were modeled as exponential current-dependent resistor with typical current–voltage characteristics of a distribution-class arrester. A high frequency model of a single-phase distribution transformer provided in the literature [2] was used in the present model without consideration of the core loss of the transformer (Fig. 3).

A Marti frequency-dependent single-core cable model was constructed with the same electromagnetic propagation characteristics as the actual cable. The Marti model is based on skin effect conductor losses, which go as the square root of frequency as do eddy current losses. In the frequency range of interest, the measured losses could be fit well with a square root of frequency dependence. The conductor conductivity was therefore adjusted so that the computed loss was close to the measured loss. As shown in Fig. 6, good agreement was obtained between the measured and modeled high frequency cable attenuations in the relevant frequency range up to about 20 MHz, which corresponds to a wavefront risetime of about 15 ns. For comparison, a reference cable model with about one order of magnitude less attenuation than TR-XLPE (or two orders of magnitude less attenuation than EPR cable) was also employed as "lossless" cable. The measured cable characteristics and model parameters which matched measured losses are given in Table I.

TABLE I
CABLE PARAMETERS

| | Velocity (m/s) | Dielectric Constant | $Z_0$ (Ω) | Conductor Resistivity (Ω-m) |
|---|---|---|---|---|
| EPR Cable: Conductor Radius, 6.6 mm; Insulation radius 18.86 mm | | | | |
| Measured | 1.6e8 | 3.6 | 33 | 2.65e-8 |
| Modeled | 1.6e8 | 3.6 | 33 | 1.018e-5 |
| XLPE: Conductor Radius, 6.2 mm; Insulation Radius, 16 mm | | | | |
| Measured | 1.85e8 | 2.6 | 35.5 | 2.65e-8 |
| Modeled | 1.85e8 | 2.6 | 35.14 | 3.05e-7 |
| Lossless Cable Conductor Radius, 6.2mm; Insulation Radius, 16 mm | | | | |
| Modeled | 1.85e8 | 2.6 | 35.14 | 1.72e-8 |

## IV. Lightning Induced Overvoltages

### A. Effect of Arrester Lead

Lightning strikes are normally modeled as current surges. The peak in the probability density distribution for lightning current is in the range of 40 kA. The current risetime can vary from about 0.1 to several $\mu$s. This current is injected into the impedance of the distribution network at the point of the strike. We assume that the lightning strikes near midspan, as shown in Fig. 2. The initial impedance seen by the lightning-induced current will be a 75 Ω, as the transient propagates down the overhead line in both directions away from the strike position. The transmitted surges propagate along the overhead line until they reach the ZnO arresters, where a change in surge impedance causes reflections and refractions. When a typical 40 kA, 0.2 $\mu$s lightning surge is injected, the lightning overvoltage waveform at the right cable termination of Fig. 2 is as shown in Fig. 1. The magnitude of the transient voltage which propagates down the cable to the transformers is mainly determined by arrester discharge voltage, the lead lengths on the arresters, and the rate-of-rise of surge current. Approximately, this voltage is the sum of arrester voltage and the arrester lead-induced voltage, which is a function of the lead length and rate-of-rise of current surge ($di/dt$). In the ideal case of no leads, the voltage propagating down to the cable is around 40 kV.

However, an arrester lead length up to 3 m is often encountered in practice. These leads produce an overvoltage due to the rate-of-rise of current propagating down the leads. Fig. 7 shows the voltage waveform across Transformer 1 (Fig. 2) for arrester lead lengths of 0, 1, and 3 m. In each case, three waveforms are shown, one for a "lossless" cable, one for a TR-XLPE cable, and one for an EPR cable. With increasing arrester lead length, the overvoltages across the transformer increases significantly. For instance, the voltage peaks of about 200 kV are produced across Transformer 1 for an arrester lead length of 3 m, which is about twice of the typical BIL (95 kV) of 15 kV class switchgear. However, high-frequency attenuation in the cable can reduce this overvoltage substantially. As is clear from Fig. 7, the greater high frequency attenuations of the EPR cable both reduces the amplitude of the initial overvoltage (the first peak in Fig. 7) and also increases the surge risetime. The EPR cable also damps the waveform very rapidly, so that by the time of the second large voltage peak for the lossless and TR-XLPE cables (around 3$\mu$s in Fig. 7), the voltage amplitude for the EPR cable is negligible. Thus, the EPR cable both decreases the impact of the first voltage peak and nearly eliminates subsequent voltage peaks.

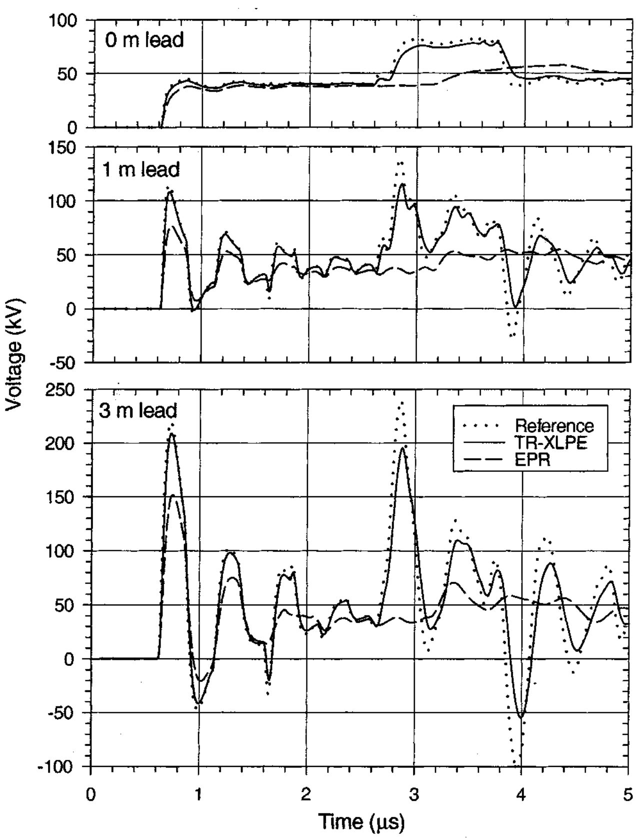


Fig. 7. Lightning-induced voltage at Transformer 1 (Fig. 2) for a 0.2 $\mu$s risetime, 40 kA lightning surge with arrester lead lengths of 0, 1, and 3 m. Reference refers to a "lossless" cable. Note that longer arrester lead lengths result in a large increase in the initial overvoltage. The attenuation of EPR cable reduces the initial transient magnitude and increases the risetime (decreases $dV/dt$) of the surge. Both of these effects will reduce the voltage across the first turns of the transformer winding. In addition, the attenuation of the EPR cable damps out reflections in the system so that the second large transient at around 3 $\mu$s becomes negligible when the system is connected with EPR cable.

## B. Effect of Surge Rate-of-Rise

The rate-of-rise of lightning current has significant influence on the level of overvoltages produced at the cable termination. We investigated this influence with a 40 kA lightning current waveform with risetimes varying from 0.1 to 1 $\mu$s. The voltage across the transformers was calculated in the case of 1-m arrester lead lengths. Fig. 8 shows the voltages across Transformer 1 (Fig. 2) for 0.1, 0.5, and 1 $\mu$s surge risetime and indicates that shorter current risetimes cause greater peak voltages and larger $dV/dt$ across the transformer. Again, EPR cable reduces the initial peak magnitude, decreases the maximum $dV/dt$ to which the transformer is exposed, and damps the surge waveform to minimize the effect of subsequent voltage peaks caused by reflections.

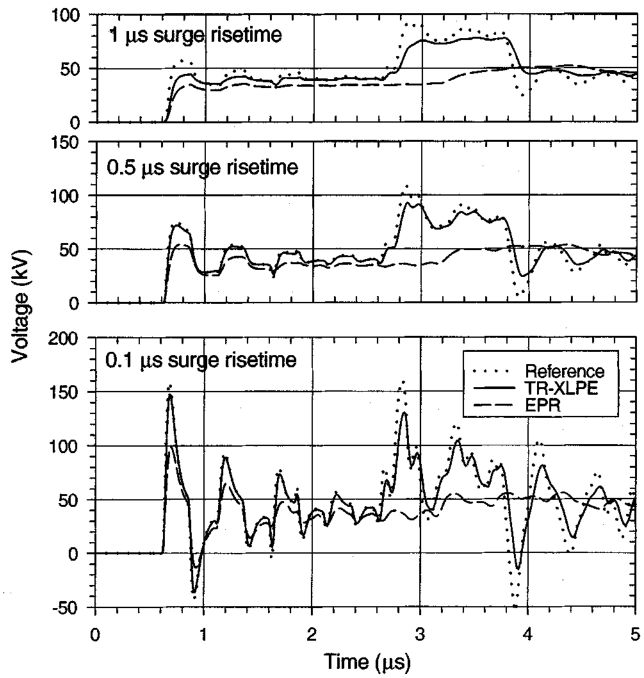


Fig. 8. Lightning-induced voltage at Transformer 1 (Fig. 2) for 40 kA lightning surge for various risetimes with an arrester lead length of 1m. With decreasing current risetime, the transient overvoltage magnitude increases as does the dV/dt of the waveform. Again EPR cable reduces the initial peak voltage and damps the waveform rapidly.

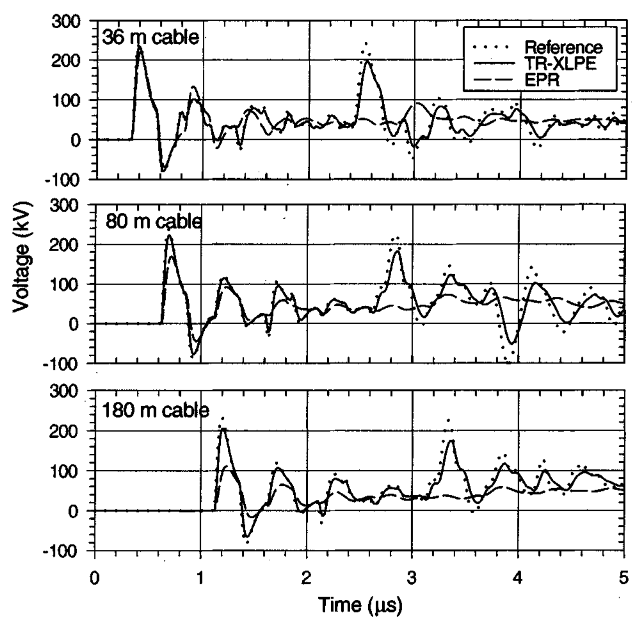


Fig. 9. Lightning-induced voltage at Transformer 1 for a 0.1 $\mu$s, 40 kA lightning surge with 2 m arrester lead length and various cable lengths. Greater cable length decreases $dV/dt$ of the initial transient. Again EPR cable damps the waveform rapidly to reduce the effect of reflections.

## C. Effect of Cable Length

The voltage across Transformer 1 was calculated as a function of cable length between the riser pole and Transformer 1. Other cable lengths were kept the same as shown in Fig. 2. Fig. 9 shows results for cable lengths of 36, 80, and 180 m. Longer cable length reduces substantially the magnitude of the first voltage peak and decreases its $dV/dt$ (increases the risetime). The subsequent strongest voltage peak results from the reflection of first peak from an open switch. The waveform travels along 192-m cable to reach the open switch, where the voltage transient is reflected back to Transformer 1. The magnitude of the resulting peak is reduced from about 200 kV for TR-XLPE to about 40 kV when EPR cable is employed.

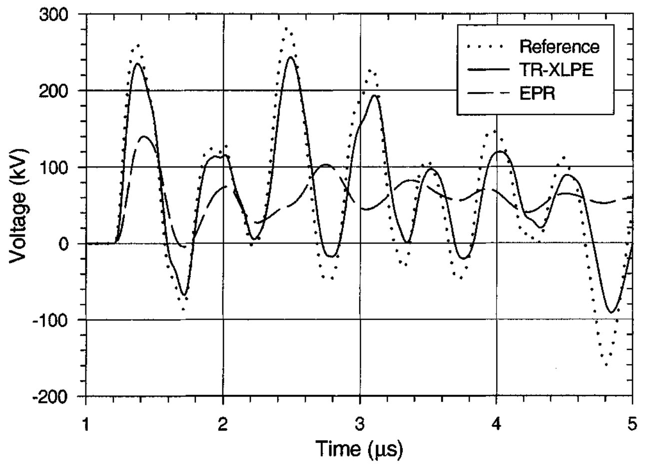


Fig. 10. Voltage across Transformer 4 (Fig. 2) for a 0.2 $\mu$s risetime, 40 kA lightning surge with 3 m arrester lead length. The reflection from the open circuit causes a series of voltage peaks which are reduced in magnitude and damped out as a function of time by EPR cable in comparison with TR-XLPE cable.

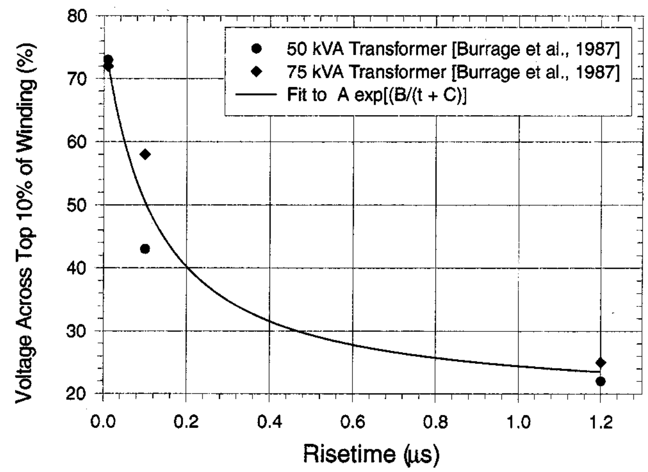


Fig. 11. Measured fraction of the voltage across the top 10% of a transformer winding for two different transformers [5] along with a curve fit to the data which is used in the present analysis.

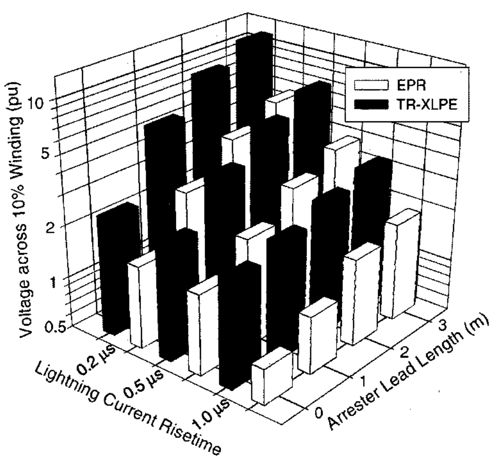


Fig. 12. Voltage in pu relative to peak line-to-ground voltage (10.78 kV) across the top 10% of the winding of Transformer 4 for a 40 kA lightning surge as a function of the lightning surge risetime, arrester lead length, and type of cable employed.

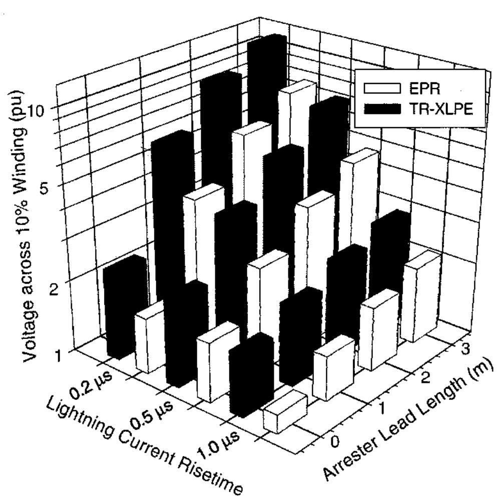


Fig. 13. Similar data to Fig. 12 except for Transformer 1.

## *D. Effect of Traveling Waves*

The reflection and refraction of the short risetime, lightning induced voltage at impedance mismatches in the system causes the voltage and $dV/dt$ across the various transformers in a network to vary. As indicated above, in the right underground branch of Fig. 2, the surge voltage is doubled at the open switch. In the left cable, Transformers 4 and 6 are located at the far ends of cables where reflection of the transient waveform from the open circuit results in higher voltages across these transformers. As shown in Fig. 10, the maximum overvoltage across Transformer 4 for a 0.2 $\mu$s risetime, 40 kA current surge and 3 m arrester lead length is about 250 kV for TR-XLPE cable. EPR cable reduces the first peak to about 120 kV and the subsequent peaks to less than the BIL of 95 kV. At the same time, the EPR cable causes the risetime to increase from about 80 ns to about 200 ns. The combination of reduced peak voltage and increased risetime (decreased $dV/dt$), will reduce considerably the turn-to-turn voltage at the top of the transformer winding.

## *E. Voltage Across First Turns of Transformer Windings*

As noted above, the high frequency attenuation of EPR cable reduces the peak magnitude and increases the risetime of voltages across the transformers connected to the cables relative to transformers connected with TR-XLPE cable. These effects combine to reduce the voltage across the first turns of the transformer. The voltage across the first turns of a transformer is a function of the surge waveform risetimes as a result of transmission line effects within the transformer winding. Fig. 11 shows data for the peak voltage across the top 10% of a transformer winding as a function of the waveform risetime. Based on computed magnitude and risetime of the first peak across transformer winding, the voltage across the top 10% of the transformer winding in pu relative to peak line-to-ground voltage was computed for a 40-kA lightning impulse with risetime of 0.2, 0.5, or 1 $\mu$s and for ZnO arrester lead lengths ranging from 0 m to 3 m. Typical results from these computations are shown in Figs. 12 and 13 for transformer 4 and 1, respectively. These data indicate that the arrester lead length, lightning current risetime, and the type of cable connecting the transformer to the overhead circuit have a large effect on the lightning induced surge voltage across the top 10% of the transformer winding. In the case of TR-XLPE cable, the top of the transformer winding is exposed to several such peak voltages per lightning impulse as a result of reflections in the system, while for the EPR cable, the transformer is exposed to only one such overvoltage as subsequent peaks are nearly completely damped by the high frequency loss of the cable.

## V. Conclusion

The computed data indicate that the type of cable employed (EPR or TR-XLPE), arrester lead length, and the rate-of-rise of lightning current have a large effect on the voltage across a transformer and the turn-to-turn voltage at the top of the transformer winding. Arrester lead lengths vary widely and are often much greater than desirable. Further, little care is taken to assure that the arrester is connected as close as possible and directly across what it is intended to protect. In the case of a connection between a cable and overhead line, the arrester is intended to protect the cable, i.e., limit the voltage between the cable conductor and cable neutral wires or tape. As such, the arrester should be connected directly between the cable conductor and cable neutral with an additional connection to the system neutral which is as short as possible.

The shorter the risetime, the larger rate-of-rise of lightning current induced overvoltages in the network. The worst case is a combination of long arrester lead and short risetime lightning currents. The industry standard 1.2 $\mu$s lightning surge risetime was set before lightning current risetimes could be measured accurately. As a result, the standard lightning surge risetime is much longer than the worst case lightning current risetime which is in the range of 0.1 $\mu$s.

The type of cable employed has a substantial impact on the overvoltages to which the transformer is subjected. A cable with large high frequency attenuation lengthens the risetime of transients as they propagate down the cable (i.e., decreases $dV/dt$) so that the voltage amplitude to which the transformer is subjected is reduced substantially. Thus, high frequency cable attenuation undoubtedly has an appreciable impact on overall system reliability, especially in areas with high incidence of lightning.

## References


[1] S. A. Boggs, F. Y. Chu, N. Fujimoto, A. Krenicky, A. Plessl, and D. Schlicht, "Disconnect switch induced transients and trapped charge in gas-insulated substations," *IEEE Trans. Power Apparat. Syst.*, Oct. 1982.

[2] A. Keyhani, S. W. Chua, and S. A. Sebo, "Maximum likelihood estimation of transformer high frequency parameters from test data," *IEEE Trans. Power Delivery*, vol. 6, pp. 858–865, Apr. 1991.

[3] S. A. Boggs, J. M. Braun, and G. C. Stone, "Attenuating voltage surges in power cable by modifying the semiconductive shields," in *Proc. IEEE Int. Symp. Electr. Insulation*, p. 491.

[4] J. M. Braun, G. C. Stone, and S. A. Boggs, "High frequency dielectric characteristics of surge attenuating semiconductive cable compounds," in *Proc. 4th Int. Conf. Conduction and Breakdown in Solid Dielectrics*, Sestri Levante, Italy, June 21–26, 1992.

[5] L. M. Burrage, E. F. Veverka, and B. W. McConnell, "Steep front short duration low voltage impulse performance of distribution transformer," *IEEE Trans. Power Delivery*, vol. 3, pp. 1152–1156, Oct. 1987.



**Li-Ming Zhou** (M'99–SM'99) received the Ph.D. degree in electrical engineering from Xi'an Jiaotong University, Xi'an, China, in 1995.

From 1995 to 1998, he visited Eindhoven University of Technology, Eindhoven, The Netherlands, Technical University of Ilmenau, Ilmenau, Germany, ABB Corporate Research Limited, Zurich, Switzerland, and the University of Oklahoma, Norman, as a Research Scientist. His past research interests have included flue gas cleaning and conversion of greenhouse gases by nonthermal electrical discharge plasma, and dielectric and arc interruption capability of $SF_6$ and its mixtures. He is an author or co-author of more than 40 technical articles and is presently with Tycom, Morristown, NJ.

**Steven A. Boggs** (F'92) received the B.A. degree from Reed College, Portland, OR, in 1968, and the Ph.D. and M.B.A. degrees from the University of Toronto, Toronto, ON, Canada, in 1972 and 1987, respectively.

He spent 12 years with the Research Division of Ontario Hydro, working in the areas of soil thermal properties, partial discharge, high field-induced degradation of solid dielectrics, and $SF_6$-insulated systems. From 1987 to 1993, he was Director of Research and Engineering at Underground Systems, Inc. He is presently Director of the Electrical Insulation Research Center and Research Professor of Materials Science, Electrical Engineering, and Physics at the University of Connecticut, Storrs, as well as an Adjunct Professor of Electrical Engineering at the University of Toronto.